Article ID: 1000-5773(2009)03-0215-08

Numerical and Experimental Study on Explosively Formed Projectile with Fins*

LIN Jia-Jian[1,2], REN Hui-Qi[1], SHEN Zhao-Wu[2]

(1. *Luoyang Institute of Hydraulic Engineering and Technology, Luoyang* 471023, *China*;
2. *Department of Modern Mechanics, University of Science and Technology of China, Hefei* 230026, *China*)

Abstract: It is a new method to produce an explosively formed projectile (EFP) with fins by attaching aluminum cover on the liner. Experimental and numerical research were performed using this new method. Furthermore, the mechanism of forming fins was discussed. The new method of forming EFP with fins was simulated by LS-DYNA, and a contrastive analysis was carried out on three typical liners, including big-cone shaped, imperfect-sphere shaped and arc-cone shaped. The results from 3D numerical simulations and experiments were also analysed. Comparison of results show that three kind of liners could form obvious fins by this new method, and the results of numerical simulations are in agreement with the experiment data. The research provides a new reference method for designing EFP with fins.

Key words: explosively formed projectile; shaped charge; fin; cover; explosive mechanics

CLC number: O385; TJ410.51 **Document code**: A

1 Introduction

With the development of sensor and electronic technology, the military target far over 200 m away could be detected and identified accurately. Therefore, the next generation of smart munitions requires explosively formed projectile (EFP) with extended standoff capability[1]. In order to defeat the difficult target at a longer standoff, the EFP must be aerodynamically stable so as to strike the target with a small miss distance and a small angle of obliquity. Because EFP with fins possesses better flight stability and higher penetration ability, a great deal of scientific studies have been carried out in every country. Many techniques of forming EFP with fins have been investigated and presented recently, such as using wave shapers embedded in explosive, profiled rind, copper shim inserted between the liner and explosives, and multi-point ignition[2-5]. The basic principle of these techniques is by changing detonation wave front structure. Because the detonation pressure of the liner depends on explosion wave, and the distribution of explosion wave on liner relies on the structure of detonation wave front. Accordingly, changing structure of explosion wave front is equal to changing detonation pressure on liner, and then the fins are formed finally.

Numerical study of multi-point ignition and profiled rind was conducted by Men, et al.[5] in 2002. He found that the two methods could form fins, but there was a lack of experimental evidence in his study. In Yu's paper[6], the test set of the EFP with fins was designed with a multi-point ignition. Simultaneously, the shape and velocities of the EFPs were measured by a flash X-ray photograph and a

* **Received date**: 2008-07-31; **Revised date**: 2008-10-12

Biography: LIN Jia-Jian(1979—), male, PhD candidate, major in explosive on mechanics. E-mail: jjlin@mail.ustc.edu.cn

SVR digital camera. A good star shaped tail and an aerodynamic stable shape were also found in his experiments. Zhao, et al. [7] used foam aluminum attaching on the liner to form fins in 2006, and they found that this new method can form EFP with fins.

Based on Zhao's research, a primary theory of forming fins is discussed. The material of cover is changed in this work. According to the results of experiments and numerical simulations, the new method of forming fins is feasible.

2 Numerical Simulation

Because of negligible influence of rind on detonation pressure[8], it is not taken into account in the numerical simulation. The structure of shaped charge includes explosive, cover and liner. Based on the simplified model, three-dimensional calculation model is established, and solid 164 is used in mesh model. The contact arithmetic is *CONTACT_SLIDING_ONLY_PENALTY among explosive, cover and liner in LS-DYNA. After 30 μs, the detonation is over, and the cover has a huge distortion, so the explosive and cover should be deleted in the later time. A detailed analysis is done in the following calculation process.

2.1 Calculation Model

In order to verify the validity of this new method, three typical liners are investigated in the numerical simulation, including big-cone shaped, imperfect-sphere shaped, and arc-cone shaped. The schematic view of three liners are shown in Fig. 1, and the physical dimensions of the liners are listed in Table 1.

Table 1 Physical dimensions of three liners

Liner type	Height of explosive h/(mm)	Diameter of explosive D/(mm)	Diameter of liner d/(mm)	Thickness of liner δ/(mm)	Radius of curvature R/(mm)	Angle of liner α/(°)
Big-cone shaped	65	50	50	3.5		146
Imperfect-sphere shaped	65	50	50	3.5	40	
Arc-cone shaped	65	50	50	3.5	50	146

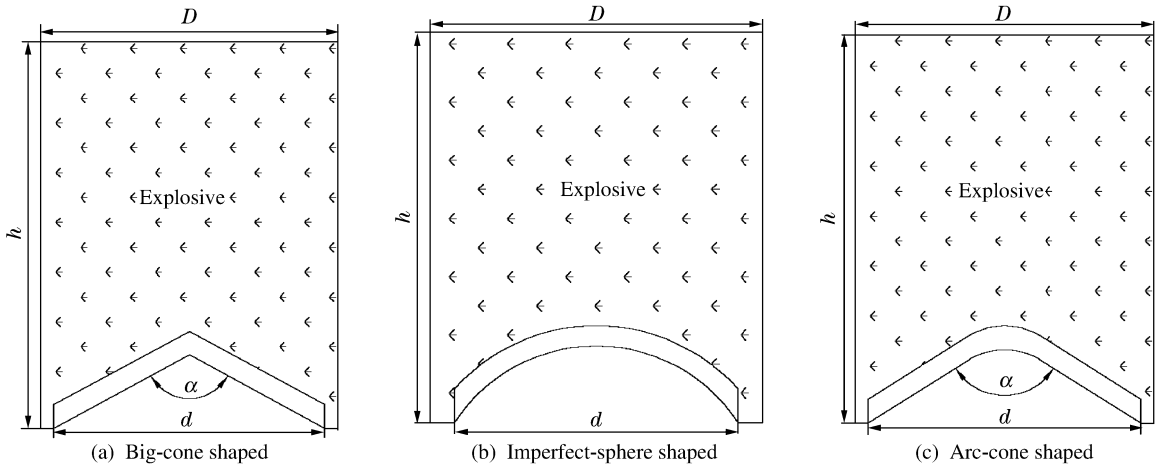


Fig. 1 Schematic view of three kind of liners

Four covers are considered in the numerical simulation, which are symmetrically placed on three kind of liners. The thickness of cover is 3.5 mm, the length is 10 mm, and the width is 8 mm.

Explosive, cover and liner are divided into three parts in mesh model, as shown in Fig. 2.

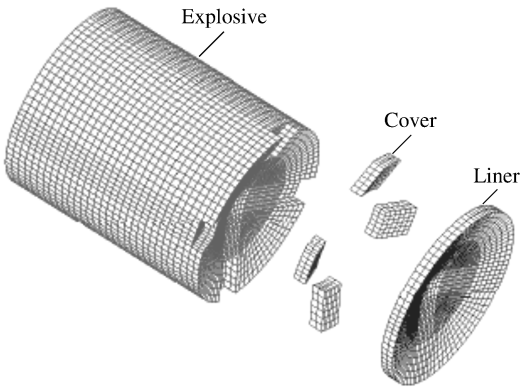


Fig. 2　Numerical model mesh

2.2　Material model

2.2.1　Explosive

Associated with JWL equation of state (EOS), MAT_HIGH_EXPLOSIVE_BURN model is used to characterise the explosive in numerical simulation. In material model, the burning coefficient shows the release of chemical energy in detonation process. The max of burning coefficient is given by

$$F = \max(F_1, F_2) \tag{1}$$

where F_1 depends on density ρ, detonation velocity D, compression ratio of volume V/V_0, and C-J pressure p_{CJ}; V depends on detonation velocity D, burning time t_b, current time t, and characteristic length of cell Δx.

If the value of burning coefficient F is over 1, set F to be 1 and keep it constant. The relation between pressure of the cell p_c and burning coefficient F is given by

$$p_c = F p_{cos}(V, E) \tag{2}$$

where p_{cos} is EOS of ralative volume V and internal energy per unit volume E.

In this paper, we employ JWL EOS to describe detonation products. Suppose that the detonation velocity is constant, JWL is defined as a function of ralative volume V and internal energy per unit volume E, and then we have

$$p_c = A\left(1 - \frac{\omega}{R_1 V}\right)\exp(-R_1 V) + B\left(1 - \frac{\omega}{R_2 V}\right)\exp(-R_2 V) + \frac{\omega E}{V} \tag{3}$$

where ω, A, B, R_1 and R_2 are parameters of the explosive, which could be obtained by experiments.

Eq. (3) can describe high explosive well. The parameters of explosive material model in numerical simulation are listed in Table 2.

Table 2　Parameters of explosive material model

ρ/(g/cm^3)	D/(km/s)	p_c/(GPa)	A/(GPa)	B/(GPa)	R_1	R_2	ω
1.84	8.835	33.70	884.5	7.678	4.600	1.350	0.250

2.2.2　Cover

The material of cover is aluminum. Mie-Grüneisen equation is adopted to describe EOS of aluminum. Johnson-Cook model is used in constitutive equation, which is given by following equation[9]

$$\sigma = (A' + B'\varepsilon_p^*)\,(1 + C\ln\dot{\varepsilon}_p^*)\left[1 - \left(\frac{T - T_{room}}{T_m - T_{room}}\right)\right] \tag{4}$$

where A', B', C are the parameters of material; ε_p^* is effective plastic strain; $\dot{\varepsilon}_p^*$ is effective plastic strain rate; T_m is melting temperature; T_{room} is room temperature. The parameters in the numerical simulation are listed in Table 3.

Table 3　Johnson-Cook parameters of aluminum

ρ/(g/cm^3)	A'/(GPa)	B'/(GPa)	C	T_m/(K)	T_{room}/(K)
2.7	0.337	0.343	0.01	877	294

2.2.3　Liner

The material of three liners is copper. Both Steinberg model and Mie-Grüneisen EOS are used in

the numerical simulation. Effects of pressure, temperature and plastic elongation are considered in Steinberg model, and then the shear modulus of liners prior to melting is given by[10]

$$G=G_0\left[1+bpv^{1/3}-h\left(\frac{e-e_c}{3R'}-300\right)\right]\exp\left(-\frac{f_e}{e_m-e}\right) \tag{5}$$

where G_0, b, h, f_e are the parameters of material; p is pressure; v is specific volume; e_c, e_m and e are cold compression energy, melting energy and specific internal energy, respectively. In Eq. (5), R' is

$$R'=R\rho/A \tag{6}$$

where R is universal gas constant, A is mole mass.

The yield strength σ_Y is expressed as

$$\sigma_Y=\sigma_0'\left[1+b'pv^{1/3}-h\left(\frac{e-e_c}{3R'}-300\right)\right]\exp\left(-\frac{f_e}{e_m-e}\right) \tag{7}$$

where σ_0' and b' are two parameters of material. The values of parameters in numerical simulation are listed in Table 4.

Table 4 The Steinberg parameters

G_0/(GPa)	b/($s^2/kg^{2/3}$)	b'/($s^2/kg^{2/3}$)	h	f	A/(g/mol)	σ_0'/(GPa)
47.7	2.83	2.83	3.77×10^{-4}	1×10^{-3}	63.55	0.12

3 Results of Numerical Simulation

3.1 Shaping of EFP with Fins

The shaping of EFP is very quick. At the time of 8 μs, the liner begin to reverse and distort because of detonation pressure. The pressure of liners exhibits several exciting differences due to four covers fixed on them. The pressure of liners' differential regions with cover is lower than that without cover. This phenomenon results in regular change of detonation pressure, and four fins are formed finally. The whole processes of three typical EFPs are obtained by numerical simulation, which are shown in Fig. (3)～Fig. (5). From these figures, we can see that three kind of liners generate symmetrical fins and the number of fins is equal to the number of covers.

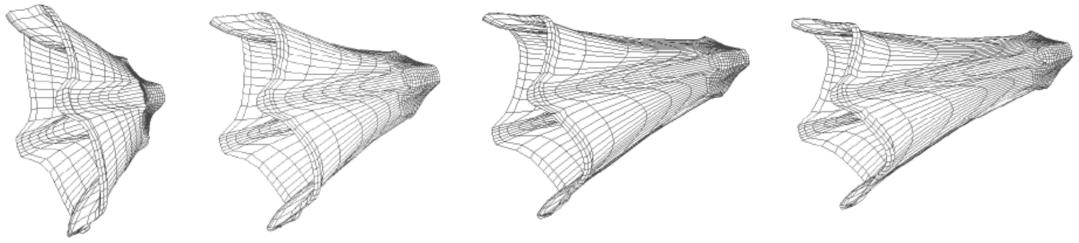


Fig. 3 EFP forming process for big-cone shaped liner

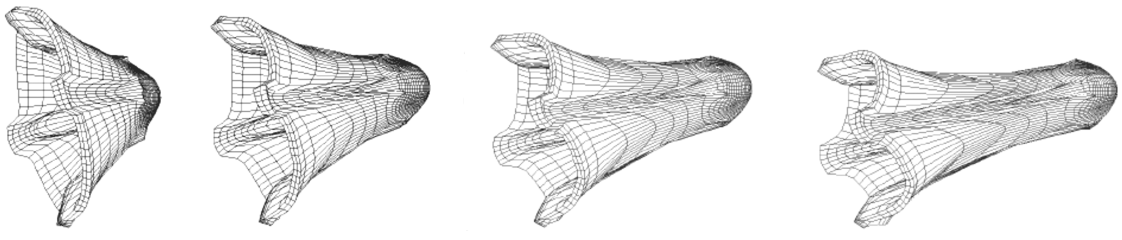


Fig. 4 EFP forming process for imperfect-sphere shaped liner

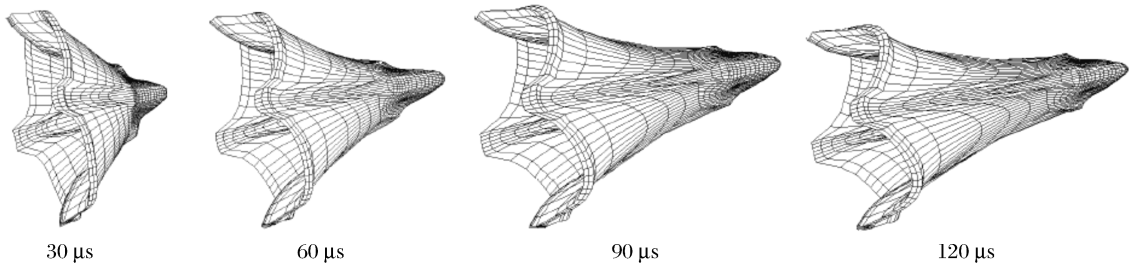


Fig. 5　EFP forming process for arc-cone shaped liner

The velocity curves of three typical liners are shown in Fig. 6. It indicates that the velocity of EFP formed from big-cone shaped liner is the highest (about 1 212.9 m/s), the velocity of EFP formed from imperfect-sphere shaped liner is the lowest (about 1 140 m/s), and the velocity of EFP formed from arc-cone shaped liner is intermediate (about 1 182.8 m/s).

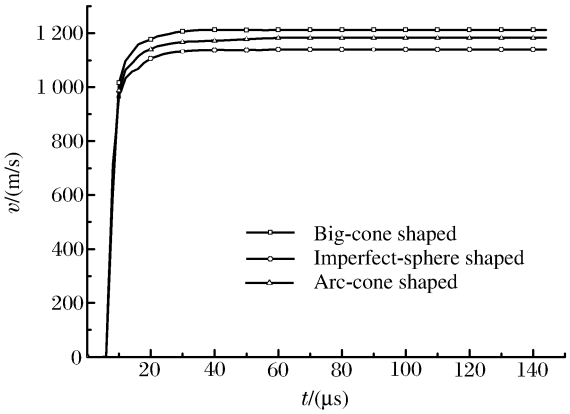


Fig. 6　Velocity history

3.2　Experimental Results

In order to study the characteristics of forming fins, the experiments of arc-cone shaped liner have been carried out. In the experiments, the physical dimensions of shaped charge are same as that in numerical simulation, and then EFPs with fins have been gained. The experiments are done in an explosive container, which is shown in Fig. 7. Schematic diagram of recovery container is shown in Fig. 8, where water is used as receiving material. A number of practices prove that water is a good material in receiving EFP.



Fig. 7　Explosive container

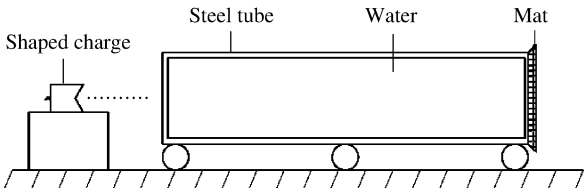


Fig. 8　Recovery container

Two EFPs with fins have been obtained, which are shown in Fig. 9. The results of experiments indicate that EFPs have four obvious fins. Because of the restriction of laboratory conditions, the covers are not precise enough in dimension, and accordingly the fins are not symmetrical perfectly. From the Fig. 9, we can also see

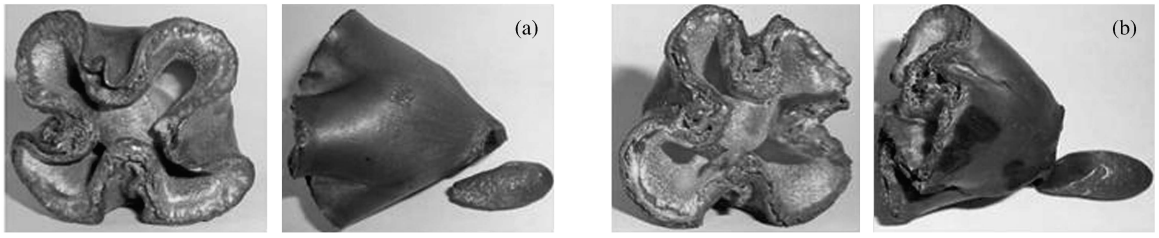


Fig. 9　Experimental results

that the top of EFPs are destroyed due to the limitation of length of the recovery container. The standoff of shaped charge is limited, so the EFPs are not completed entirely, and then the aspect ratio is smaller than that of numerical simulation. The detailed parameters of EFPs are listed in Table 5.

Table 5 Parameters of EFPs

Type	Minimum diameter of EFP D_1/(mm)	Maximum diameter of EFP D_2/(mm)	Length of EFP L/(mm)	L/D_1	L/D_2
Big-cone	11.6	27.5	43.7	3.8	1.6
Imperfect-sphere	11.4	29.5	40.9	3.6	1.4
Arc-cone	11.7	28.2	38.6	3.3	1.4
Arc-cone experiment-1	12.2	25.4	33.8	2.8	1.3
Arc-cone experiment-2	13.6	23.5	30.6	2.3	1.3

4 Mechanism of Forming EFP with Fins

The essential principle of the new method is by changing the configuration of detonation wave. When explosion pressure is changed, the pressure on liner is also regularly changed. To further investigate the mechanism of forming EFP with fins, the collapse velocity and the pressure of liners are discussed separately.

4.1 The Collapse Velocity of the Liner

Provided that the explosive is detonated entirely in a extremely short interval of time, the rarefaction wave will spread in detonation products along the normal of the shaped charge surface. The self-closing movement of the liner results in adiabatic expansion work of the effective shaped charge. The collaps velocity of the liner can be deduced from adiabatic-compression method and momentum conservation, which is given by

$$v_{0i}=\frac{D}{2}\left\{\frac{\rho_e b_{ei}}{2\rho_j b_i}\left[1-\left(\frac{b_{ei}\cos\dfrac{\beta_i+\alpha}{2}}{l_{mi}\sin\alpha+b_{ei}\cos\dfrac{\beta_i+\alpha}{2}}\right)^2\right]\right\}^{1/2} \tag{8}$$

where D is the detonation velocity of explosive, ρ_e is the effective shaped charge, b_{ei} is the thickness of effective shaped charge at the i-cell, ρ_j is the density of liner, b_i is the thickness of liner at the i-cell, l_{mi} is the generatrix length of liner at the i-cell, α is half angle of cone, β_i is liner collapse angle.

Five cells from the liner are selected as research objects, which are shown in Fig. 10. The velocity curves of these cells can be obtained by numerical simulation, which are shown in Fig. 11～Fig. 13. Contrasting these velocity curves of three kind of liners, we can see that they are similar. The velocity of A is the lowest on account of the cover. The velocity of C, D and E are the highest, because the detonation wave arrives at the top of liner first. B-cell is situated on the edge of the liner, so its velocity is higher than A and lower than C.

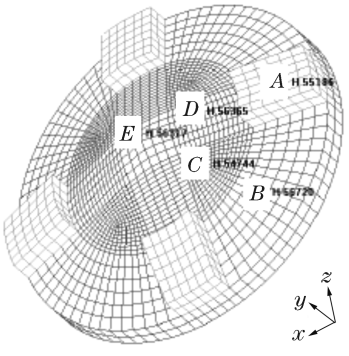


Fig. 10 Liner mesh

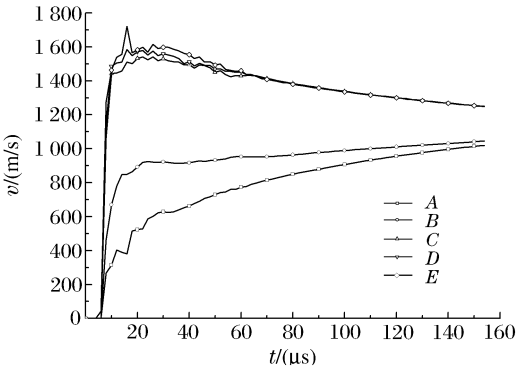


Fig. 11 Velocity history of big-cone shaped liner

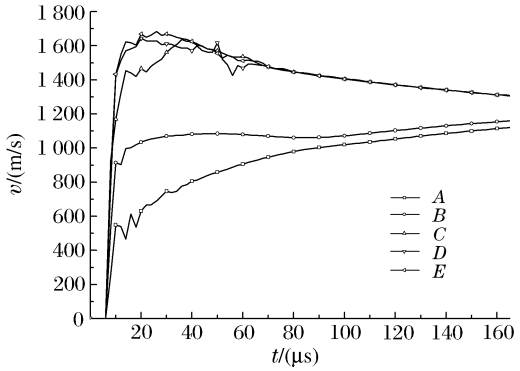


Fig. 12　Velocity history of imperfect-sphere shaped liner

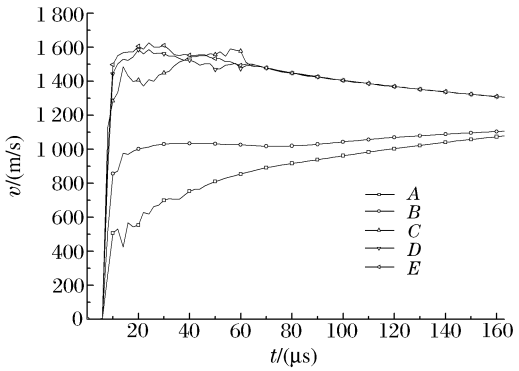


Fig. 13　Velocity history of arc-cone shaped liner

4.2　Attenuation of shock wave in cover

Regular change of the pressure on liner results in regular distortion, thereby forming of the fins. It is difficult to give theoretical expression because of the complexity of shock wave in the attenuation. The expirical formula is adopted in the projected range of the cover thickness, which is expressed as

$$p' = p_c \exp(-ax) \tag{9}$$

where p_c is the pressure of the cell, p' is the pressure at the location of x on the cover, a is the attenuation coefficient of shock wave in cover, x is the thickness of cover.

Just similar to the velocity analysis, five cells are selected as research objects, and their pressure curves are obtained, which are shown in Fig. 14 ~ Fig. 16. Contrasting the five pressure curves of three typical liners, we found that the pressure curves were similar, too. The pressure of A is lower than B due to the cover adhering to the liner, and the shock wave is attenuated in the cover. The pressure curve of C, D and E are similar, because three cells are close to each other. The distortion velocity of A is different from that of B, therefore the negative pressure appears in A.

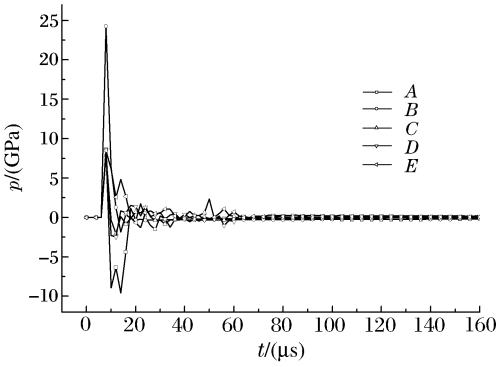


Fig. 14　Pressure history of big-cone shaped liner

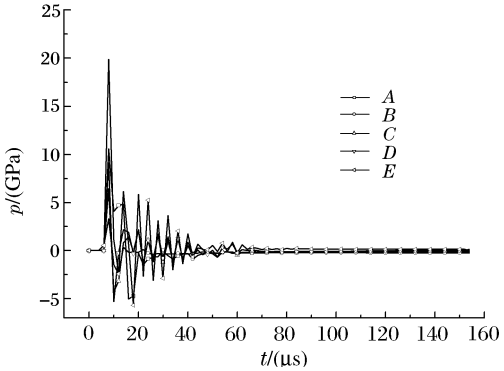


Fig. 15　Pressure history of imperfect-sphere shaped liner

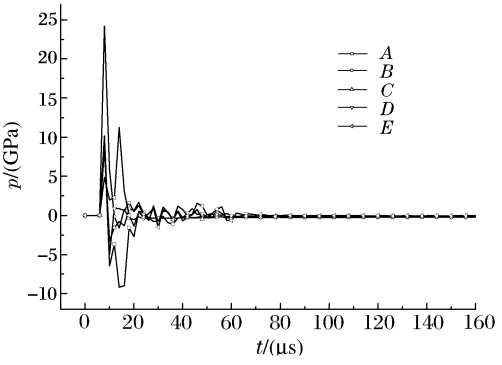


Fig. 16　Pressure history of arc-cone shaped liner

5　Conclusions

A new method of forming EFP with fins was simulated by LS-DYNA, and a contrastive analysis was

carried out on three typical liners, including big-cone shaped, imperfect-sphere shaped and arc-cone shaped. The results show that three kind of liners could form obvious fins by this new method, and the number of fins is equal to the number of the covers. Combining with the experiments of arc-cone shaped charge, the results validate the feasibility of the new method. Moreover, according to the effect of variation of collapse velocity and detonation pressure on liners, the mechanism of forming fins was discussed.

References:

[1] Bender D, Chhouk D, Fong R. Explosively Formed Penetrators (EFP) with Canted Fins [A]//19th International Symposium on Ballistics [C]. Interlaken, Switzerland, 2001: 7-11.

[2] Bouet T H, Tarayre P, Guillon J P. Study of a Multi-Point Ignition EFP [A]//15th International Symposium on Ballistics [C]. Israel, 1995: 159-166.

[3] Joseph C, David E B, Richard F. A Unique Method of Providing an Explosively Formed Penetrator with Fins [A]//17th International Symposium on Ballistics [C], Midrand: The South African Ballistics Organisation Press, 1998: 55-62.

[4] Weimann K. Flight Stability of EFP with Star Shaped Tail [A]//15th International Symposium on Ballistics [C]. Queber, Canada, 1993: 755-763.

[5] Men J B, Jiang J W, Wan L Z. 3D Numerical Simulation Research on the Formation of Explosively Formed Penetrator with Fins [J]. Journal of Beijing Institute of Technology, 2002, 22(2): 166-168. (in Chinese)
门建兵, 蒋建伟, 万丽珍. 带尾翼 EFP 形成的三维数值模拟研究 [J]. 北京理工大学学报, 2002, 22(2): 166-168.

[6] Yu C, Dong Q D, Sun C W, et al. The Experimental Formed Projectile with Star Shaped Tail [J]. Explosion and Shock Waves, 2003, 23(6): 561-564. (in Chinese)
于 川, 董庆东, 孙承纬, 等. 带尾翼翻转型爆炸成型弹丸试验研究 [J]. 爆炸与冲击, 2003, 23(6): 561-564.

[7] Zhao H Y, Shen Z W, Li C B, et al. A New Way of Explosively Formed Projectile with Stabilizing Fins [J]. Chinese Journal of Energetic Materials, 2006, 14(2): 102-104. (in Chinese)
赵慧英, 沈兆武, 李成兵, 等. 带尾翼爆炸成型弹丸的新技术 [J]. 含能材料, 2006, 14(2): 102-104.

[8] Zhao H Y. Research on Technology of Fin Stabilized EFP [D]. Hefei: University of Science and Technology of China, 2007. (in Chinese)
赵慧英. 尾翼稳定爆炸成型弹丸相关技术研究 [D]. 合肥: 中国科学技术大学, 2007.

[9] LS-DYNA Keyword User's Manual [M]. California: Livermore Software Technology Corporation, 2001.

[10] Steinberg D J. Equation of State and Strength Properties of Selected Materials [M]. Lawrence Livermore National Laboratory, 1991.

尾翼型爆炸成型弹丸的数值模拟及实验研究

林加剑[1,2], 任辉启[1], 沈兆武[2]

(1. 洛阳水利工程技术研究所, 河南 洛阳 471023;
2. 中国科学技术大学近代力学系, 安徽 合肥 230026)

摘要: 在药型罩上粘附铝隔板是一种新的形成尾翼型爆炸成型弹丸(Explosively Formed Projectile, EFP)的实验方法。通过实验和数值模拟对该方法进行了分析, 探讨了形成尾翼的机理。利用有限元分析软件 LS-DYNA, 对大锥角型、球缺型和弧锥结合型 3 种不同药型罩在采用新方法时形成的尾翼型 EFP 进行了三维数值模拟分析, 并将模拟结果与实验结果进行对比。研究结果表明: 3 种药型罩均能形成比较明显的尾翼, 数值计算结果与实验结果较吻合。该研究为设计尾翼型 EFP 提供了一种新的参考方法。

关键词: 爆炸成型弹丸; 聚能装药; 尾翼; 隔板; 爆炸力学

中图分类号: O385; TJ410.51 **文献标识码:** A